Control of an Electromagnetically Actuated Resonance Punch

M. Ahrens, T. Hasselbusch, M. Dagen, B.-A. Behrens, T. Ortmaier

ABSTRACT

In the area of metal forming the production of micro-components in huge quantities by cutting plays a central role. These components are often manufactured on modified mechanical high speed presses with stroke rates of up to 4,000 strokes per minute (spm) and punching forces of up to 2,000 kN. In terms of maximum cutting force and overall size of the punching machine, this may represent a significant oversizing, depending on the application. A better adaptability of the machine to the process could reduce production cost by lower space and energy consumption. To fulfill both requirements, a prototype of an electromagnetically driven punch machine with highly efficient resonance drive and miniaturization potential has been built at the Mechatronik Zentrum Hannover (MZH). The ram consists of a mass-spring system and is brought into resonance oscillations by an electromagnetic actuator. An advantage of this resonance propulsion is that only magnets with low nominal force are needed, since only small forces are necessary to replenish the energy lost by friction and the cutting process. A central role in this setup plays the power amplifier, which controls the magnet's current. To achieve an optimal control performance under various hardware conditions, different energy-based control approaches are proposed in this paper.

1 INTRODUCTION

In the area of metal forming, the production of micro-components in quantity takes place on mechanical speed presses with modified drive kinematics. These presses provide stroke rates of up to 4,000 strokes per minute (spm) and punching forces up to 2,000 kN. Since micro-components usually do not require high cutting forces, many production machines may be oversized both in terms of maximum cutting force and size. As a consequence, production costs increase due to higher space and energy consumption. This could be improved by a better adaptability of the machine to the process.

Several research projects analyzed alternative concepts for production of micro-components. A European team deployed piezo actuators in a micro piezo press [1]. An alternative is the usage of electromagnets. This has already been studied in various designs [2–4]. These approaches provide a high cutting velocity, which is necessary for a good workpiece quality, but only provide stroke rates up to 350 spm. The Schuler AG developed a punch machine known as Stanzrapid [5–7] which uses linear motor drives to force the plunger through the metal sheet. Thus, stroke rates of up to 1,200 spm and forces up to 40 kN are possible. A drawback is the poor efficiency, which demands for an external cooling unit. Another approach pursued by the MZH is an electromagnetically actuated punch machine. It uses multiple electromagnetic actuators for cutting and additionally to achieve an active tilt compensation [8–11]. This machine stands out against others because of its small installation space. It requires significantly less space compared to common punch machines [12, 13]. The authors of this paper modified the concept of the MZH and built an electromagnetically actuated resonance punch machine. It uses the magnets of the machine presented in [8], but uses a highly efficient control concept allowing further miniaturization and higher energy efficiency [15]. The punch machine differs from previous approaches with direct magnetic drive in one key aspect: The resonance propulsion concept requires very low actuator force resulting in smaller machine dimensions. In contrast to common punch machines, the drive's nominal force does not meet the force required for the actual cutting process. Instead, the energy is added during the whole stroke period and is converted into cutting force. Summarizing, this concept combines a cheap and energy efficient drive with a compact space-saving construction while providing high stroke rates. An optimal utilization of the magnets demands for sophisticated control methods, which are proposed in this paper.

The paper is organized as follows: After presenting the concept and essentials, four control methods are proposed. These methods are compared is terms of performance and practical use, based on simulation results.

2 CONCEPT

Fig. 1 shows the concept of the direct drive kinematics utilizing a high performance electromagnet and a mass-spring system with low damping. The ram is located between the upper and the lower baseplate and is able to oscillate in vertical direction. The electromagnet, located below the upper baseplate, excites oscillations of the ram. However, its rated force is much lower than the required cutting force.

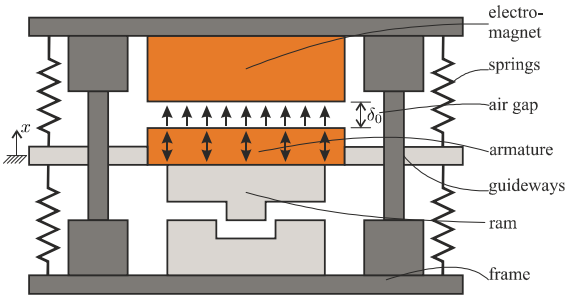

Fig. 1 Sketch of concept

The basic idea is to excite the mass-spring at its resonance frequency. Before the machine is able to cut through the workpiece, a swing-up process is necessary to store enough energy in the system. A control algorithm calculates the actual energy stored in the system, compares it to a target value and calculates an according current for the actuators. In this way, the ram is excited to small oscillations, rising till the target amplitude and energy is reached, cf Fig. 2.

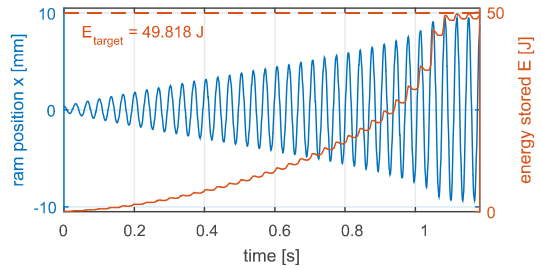

Fig. 2 Simulated starting process of the machine

Once the desired stroke amplitude is reached the mass spring system holds enough energy for a cutting process and the workpiece can be fed into the machine. During the cutting process energy dissipates out of the system and has to be replenished during the next stroke. To keep the reduction in the amplitude small, it is necessary to store more energy than needed for one stroke. Fig. 3 depicts the energy flux over one stroke period's duration.

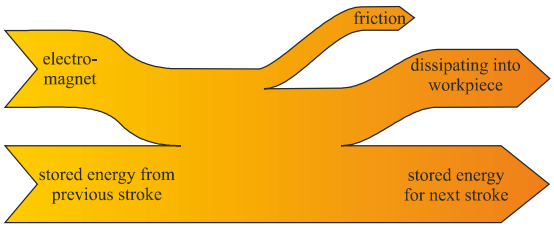

Fig. 3 Energy flux diagram over one stroke period

The benefit of the resonance propulsion is the low nominal force of the magnet because the energy needed for the punch process is stored in the springs and the mass of the ram:

$$E = \frac{1}{2}cx^2 + \frac{1}{2}m\dot{x}^2. \qquad (2)$$

$$x = \delta_0 - \delta$$

In this equation, c is the spring stiffness, δ the actual air gap, m and $\dot{\delta}$ the ram's mass and velocity and δ_0 the air gap at idle position. The stroke rate can be adjusted by the spring stiffness c and ram mass m. Thus, a modular setup is possible, were the operator can choose between different sets of springs or additional weights that can be mounted on the ram. The calculations and experiments presented in this paper were executed with a ram mass m of 100 kg, a spring stiffness c of 1.1 $\frac{\mathrm{kN}}{\mathrm{mm}}$ and an airgap δ_0 of 10 mm. The system design is discussed in detail in [15].

3 SYSTEM CONTROL

Due to high nonlinearity of the magnets force characteristics and the dynamics of the electrical system, the system is controlled at a frequency of 10 kHz. For the proposed control methods, an accurate position and velocity measurement is needed. While the sensor provides high resolution and accurate position measurement, small oscillations of the sensor mounting cause distorted velocity signal obtained by derivation. Thus, an Extended Kalman Filter (EKF) is implemented for position and velocity estimation. Therefore, the calculation of the control variable E using the estimated states x and $\dot{x}$ with low distortion and noise is possible.

3.1 ACTUATOR DESIGN AND CALCULATION

The energy added by the magnet to the system can be calculated by integration of the magnet's force along the moving path of the ram. This path starts at the lowest point of the oscillation δ_1 and ends on the highest point at $\delta_2 = \delta_{\text{target}} = 0.5$ mm. For safety reasons, the value of δ_2 should not be closer to zero, to take saturation and nonlinearity effects into account. The maximum energy the magnet can add to the system during a stroke period is the integral of the force

$$F_{\text{mag}} = \frac{n^2 I_{\text{max}}^2 \mu_0 A}{8\delta^2} \tag{3}$$

along the air gap:

$$W_{\text{mag}} = \int_{\delta_1}^{\delta_2} F_{\text{mag}} \mathrm{d}\delta = \frac{n^2 I_{\text{max}}^2 \mu_0 A}{8} \left(\frac{1}{\delta_1} - \frac{1}{\delta_2}\right), \tag{4}$$

where n represents the number of windings of the magnet, I_{max} the maximal current, μ_0 the magnetic permeability of vacuum, A the effective surface area of the magnet and δ the air gap between magnet and ram.

Depending on the control method, a high dynamic of the force and therefore the current, is required, especially at the ram's peak position. Because of the high inductivity at low air gaps, the current changes relatively slow. Thus, the dynamic of the electrical system cannot be neglected and is analyzed in the following.

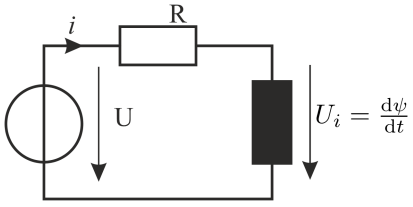

Fig. 4 Electrical schematic of a magnet

The magnet is driven by a controller supplied by an intermediate circuit of 600 V. Therefore the dynamics behavior is mainly determined by the inductivity. The electrical schematic of an electromagnet, depicted in Fig 4. can be mathematically described by:

$$U = Ri + \frac{\mathrm{d}\Psi}{\mathrm{d}t}. \tag{5}$$

The magnetic flux density and linked magnetic flux is given by

$$\begin{aligned} B &= \frac{ni\mu_0}{2\delta}, \\ \Psi &= nB \cdot \frac{A}{2}. \end{aligned} \tag{6}$$

The time derivative of the linked magnetic flux in the magnet gives the induced voltage in the magnets coil:

$$U = Ri + \frac{\mathrm{d}}{\mathrm{d}t}\left(\frac{n^2 i \mu_0 A}{4\delta}\right). \tag{7}$$

Based on those equations, in the following different control methods are developed and compared.

3.2 ENERGY-BASED BANG-BANG-CONTROL

A simple approach for operating the punch machine is an energy-based approach in combination with a bang-bang-control. It calculates the energy E_{com}, which is stored in the system, and compares it to the target value E_{target}, which is calculated from the target tude δ_{target}. If the ram is moving towards the magnet and thus, energy can be added to the system, the magnet applies the maximum force F_{max} with the current I_{BB} onto the ram, as long as the target energy has not been reached. The following equations describe the controller:

$$E_{\text{com}} = \frac{1}{2} c (\delta - \delta_0)^2 + \frac{1}{2} m \dot{\delta}^2, \tag{8}$$

$$E_{\text{target}} = \frac{1}{2} c \left(\delta_{\text{target}} - \delta_0\right)^2, \tag{9}$$

$$I_{\text{BB}} = \begin{cases} 0 & \text{for } E_{\text{com}} \geq E_{\text{target}} \wedge \dot{\delta} \geq 0 \\ I_{\text{max}} & \text{for } E_{\text{com}} < E_{\text{target}} \vee \dot{\delta} < 0 \end{cases}. \tag{10}$$

While this method is simple to implement, there are some drawbacks. Fig 5. shows the current and ram's position during one oscillation period in simulation. It can be seen, that the high induction effects reduce the current below its target value. Furthermore, the current drops not immediately to zero once the target energy is reached. Particular at the end of the oscillation period, when the air gap gets small, the inductivity of the magnet is very high and rapid current changes demand for high voltage, which in this case is limited to 600 V. Thus, the magnets force is applied to the ram longer than necessary causing an overshoot of the oscillation amplitude.

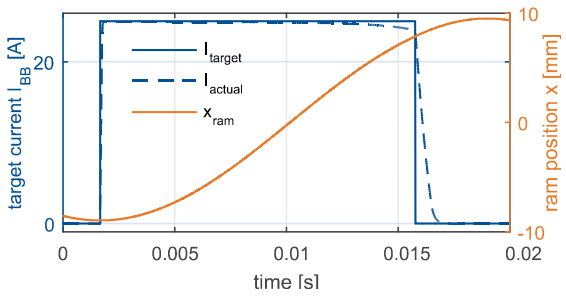

Fig. 5 Current and ram position with bang-bang-control

Since the punching process is a cyclic process, an iterative learning control (ILC) can be applied to counteract the overshoot. However, this does not prevent the first overshoot and causes problems dealing with changing disturbance forces. As a punching process inherits its high disturbance forces caused by the metal sheet, this control method is not able to utilize the full potential of the machine.

3.3 ENERGY-BASED BANG-BANG-CONTROL WITH 'FREERUN'

To improve the performance of the bang-bang controller, the energy stored in the magnetic field in the airgap can be taken into account. Once the cumulated energy (potential and kinetic energy of the ram as well as the magnetic field energy of the air gap) reaches the target energy, the voltage applied on the solenoids is switched to zero. Using the voltage instead of the current as control variable avoids the delay of the system 'magnet' in the controller; changes of the voltage come into effect immediately. A drawback is the necessity of a 'freerun-mode' in the current amplifier, which controls the magnets current. In this mode, the control voltage is zero and the current can flow through the amplifier, only being reduced by the ohmic resistance of the solenoids and induction effects. The following equations describe the controller:

$$E_\delta = \iiint_V \frac{BH}{2}\,\mathrm{d}V = \frac{n^2 i^2 \mu_0 A}{8\delta}, \qquad (11)$$

$$E_{\mathrm{com,FR}} = \frac{1}{2}c(\delta - \delta_0)^2 + \frac{1}{2}m\dot{\delta}^2 + E_\delta, \qquad (12)$$

$$I_{\mathrm{FR}} = \begin{cases} 0 & \text{for } \dot{\delta} \geq 0 \\ I_{\max} & \text{for } E_{\mathrm{com,FR}} < E_{\mathrm{target}} \wedge \dot{\delta} < 0 \\ \text{freerun} & \text{for } E_{\mathrm{com,FR}} \geq E_{\mathrm{target}} \wedge \dot{\delta} < 0 \end{cases} \qquad (13)$$

When the ram moves towards the magnet, field energy is converted to kinetic energy. This occurs by a voltage induced into the solenoids, cf. (5) which reduces the current. During the 'freerun-mode' this energy is not replenished by the amplifier's power supply causing the current to decrease. Once the ram's velocity reaches zero, the amplifier pulls out the remaining current.

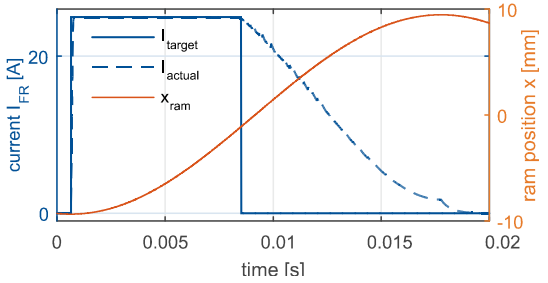

Fig. 6 Current and ram position with 'freerun-control'

Fig. 6 shows the target and actual current as well as the ram's position. During the 'freerun-mode' the target current is set zero while the actual current decreases steadily.

This control method results in a robust operation, since overshoots are prevented effectively in this way. Besides the model parameter, no controller parameter has to be adjusted for this method. On the other hand, the target amplitude cannot be reached by design, because of the remaining field energy in the target air gap. However, this effect is quite small and the advantages of this approach compensate for this flaw.

3.4 ENERGY-BASED PI-CONTROL

Another control method is a standard energy-based PI-control. When the ram moves towards the magnet, the target current composes of a term proportional to the control error ϵ and a integral term weighting the control error over time. This approach has the advantage, that the target current decreases towards the end of the oscillation period, when the control error gets smaller. In this way, the current gradient is smaller in comparison to the bang-bang-control, making it easier for the current amplifier to follow the target value, reducing the overshoot in position amplitude. The control error and the target current can be calculated by the following equations:

$$\epsilon = \left(E_{\mathrm{target}} - E_{\mathrm{com}}\right), \qquad (14)$$

$$I_{\mathrm{PI}} = \begin{cases} 0 & \text{for } \dot{\delta} \geq 0 \\ k_{\mathrm{P}}\epsilon + k_{\mathrm{I}} \int \epsilon \,\mathrm{d}t & \text{for } \dot{\delta} < 0 \end{cases}. \qquad (15)$$

The performance of the PI-control heavily depends on the adjustment of the control parameters k_P and k_I. Too high values result in a similar behaviour as the bang-bang-control, too small values cause the ram not to reach its target amplitude. Fig. 7 shows the current and ram's position during one oscillation period using the PI-control.

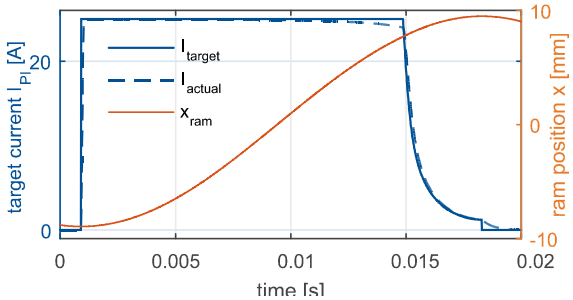

Fig. 7 Current and ram position with PI-control

3.5 CURRENT-OPTIMAL CONTROL CONSIDERING THE SPRINGS CHARACTERISTICS

High amplitudes and steep flanks of the desired current cause most of the problems in controller performance, i.e. overshoots and noise generation. A controller only applying the minimal necessary current while utilizing the whole time window can avoid these issues. This approach suffers under the flaw, that the ram has to hurdle a critical point x_S, where the springs generate more force than the magnet. Since this point depends from the solenoids current, air gap and velocity, it makes sense to describe this control method using energy calculations.

A controller, that applies the minimum current, has to add at least that amount of energy to the system to hurdle the critical point x_s. During the interval $[x_\mathrm{start}, x]$, the magnet can add the energy

$$E_\mathrm{mag} = \frac{n^2 i^2 \mu_0 A}{8}\left(\frac{1}{\delta_0 - x} - \frac{1}{\delta_0 - x_\mathrm{start}}\right) + E_\mathrm{com} \qquad (16)$$

to the system, where the energy E_com is the energy already stored in the system.

The energy E_c necessary to compress the springs is calculated by

$$E_\mathrm{c} = \frac{1}{2} c x^2. \qquad (17)$$

Fig. 8 shows the energy functions E_mag at a current of 10 A respectively 25 A and E_c starting with an energy of 32 J at x_start= 0 mm.

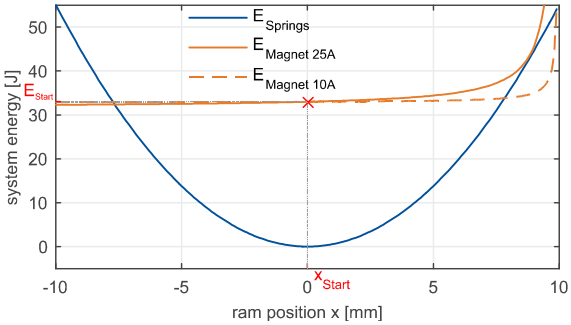

Fig. 8 Energy functions of springs and electromagnet

If the current is to low, the energy functions intersect between the actual position x_start and the desired position x_target. At an intersection point, the ram stops moving towards the magnet and the springs are pushing the ram in the opposite direction. Thus, the ram does not reach smaller air gaps, where the magnet is able to generate much higher forces.

This results in the demand, that values of both energies must not intersect, which results in a third-order polynomial:

$$E_\mathrm{c} - E_\mathrm{mag} = a_3 x^3 + a_2 x^2 + a_1 x + a_0 \overset{!}{=} 0, \qquad (18)$$

$$\begin{aligned} a_3 &= -4c\delta_0 + 4cx_\mathrm{start} \\ a_2 &= -4c\delta_0^2 + 4c\delta_0 x_\mathrm{start} \\ a_1 &= -n^2 i^2 \mu_0 A + 8E_\mathrm{com}\delta_0 - 8E_\mathrm{com} x_\mathrm{start} \\ a_0 &= n^2 i^2 \mu_0 A x_\mathrm{start} - 8E_\mathrm{com}\,\delta_0^2 + 8E_\mathrm{com}\delta x_\mathrm{start}. \end{aligned} \qquad (19)$$

Instead of solving the equation directly, it is possible to determine the graph's shape by calculating its discriminant D, cf. Table 1.

	Solution of the cubic equation
$D > 0$	One real, two complex conjugate solutions
$D = 0$	Three real solutions, at least two equal solutions
$D < 0$	Three different real solutions

Tab. 1 Solutions of third-order polinomial

If the discriminant equals zero, the energy functions touch in the point x_s:

$$p = \frac{a_1}{a_3} - \frac{a_2}{3a_3}, \qquad q = \frac{2a_2^3}{27a_3^3} - \frac{a_2 a_1}{a_3^2} + \frac{a_0}{a_3}, \qquad (20)$$

$$D_\mathrm{E} = \left(\frac{p}{3}\right)^3 + \left(\frac{q}{2}\right)^2 \overset{!}{=} 0. \qquad (21)$$

This equation depends on the magnets current. Collecting the factors of the current leads to the sixth-order polynomial

$$D_{\mathrm{E}} = b_6 i^6 + b_4 i^4 + b_2 i^2 + b_0. \qquad (22)$$

This equation can be solved analytically, substituting the even numbered powers of the current and using Cardano's method. The axial symmetry of the equation is caused by the fact, that the direction of the magnet's current has no influence on the direction of the resulting force. The minimal needed current I_{min} to reach the target amplitude is the smallest real solution of the polynomial.

This method prevents intersections of the energy functions and prevents the ram from being pushed back until the critical point x_{s} is hurdled. Beyond this point, the current would decrease, because the force slope of the magnet is higher than that of the springs. The current needed to reach the target energy can be derived from equation (9):

$$I_{\mathrm{mag}} = \frac{8(E_{\mathrm{target}} - E_{\mathrm{com}})}{n^2 \mu_0 A \left(\frac{1}{\delta_0 - x} - \frac{1}{\delta_0 - x_{\mathrm{start}}} \right)}. \qquad (23)$$

The target current can be calculated using (24) or amplitudes beyond the critical point:

$$I_{\mathrm{opt}} = \begin{cases} 0 & \text{for } \dot{\delta} \geq 0 \\ I_{\mathrm{min}} & \text{for } I_{\mathrm{min}} > I_{\mathrm{mag}} \wedge \dot{\delta} < 0 \\ I_{\mathrm{mag}} & \text{for } I_{\mathrm{min}} \leq I_{\mathrm{mag}} \wedge \dot{\delta} < 0 \end{cases}. \qquad (24)$$

This control approach utilizes the complete window where the magnet is capable of adding energy to the system. Therefore, the required target current is minimized.

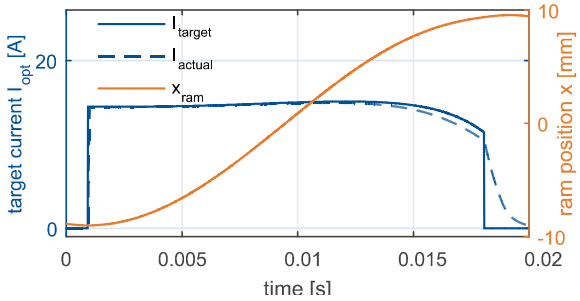

Fig. 9 Current and ram position with current-optimal-control

Adding a small offset to the current will cause the magnet to add more energy to the system than required. Thus, the current will decrease towards the end of the period, avoiding a steep flank when the target amplitude is reached, cf. Fig. 9.

4 RESULTS

The presented control methods differ in complexity, hardware requirements and performance. Therefore, the concepts are compared in the following sections.

4.1 STARTING PROCESS

The core of the compact and energy saving concept of this resonance punch is the small drive unit in comparison to the rated punch force. The small magnet is not able to pull the ram directly up to the target amplitude. Instead, the ram is excited at its resonance frequency using one of the control methods described before. Fig. 2 shows the starting process using the bang-bang-controller with 'freerun-mode' to achieve the target energy of approx. 50 J equal to 9.5 mm amplitude. With that amount of energy, the punch would be able to use approx. 15 J for cutting. All control approaches converge to the bang-bang-control during the starting process, because of the current limitation.

4.2 FULL AMPLITUDE OPERATION

At the time the target energy is reached, the control approaches differ significantly. As mentioned before, the magnets dynamics are a big disturbing factor, which hinders the controller to apply the target current to the systems. Figure 10 compares the simulated target current of the different control methods and the actual current.

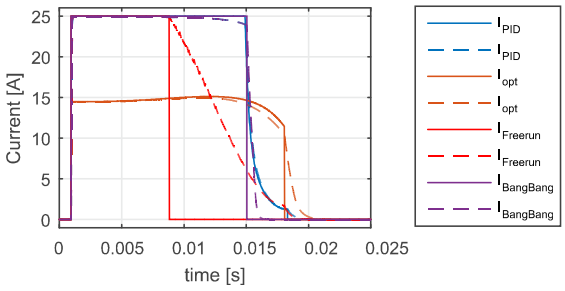

Fig. 10 Comparison of the target currents of the different control methods

Especially the bang-bang-control applies high currents and steeps current flank, resulting in overshoots of the ram's amplitude. The flanks of the PI-controller's target current are not as steep but it applies also high currents at low air gaps, putting high requirements on the current amplifier. The bang-bang-control with 'freerun-mode' shows the best performance, since stew flanks are avoided completely and energy losses are minimized. The current calculated

by the current-optimal control puts the lowest demands on the current amplifier, since it is low in amplitude and has low slope rates while showing good performance. However, when the system is pushed to its limit and high currents are applied, stew current flanks cannot be avoided and the 'freerun-mode' control is still the better choice.

5 CONCLUSION AND OUTLOOK

In this paper, several control methods for an electromagnetically driven punch machine are presented and discussed. The machine design enables reduction of installation space and energy consumption. To optimize the machine performance, advanced control algorithms are needed. The developed control methods are evaluated in terms of requirements on the current amplifier and control performance.

An energy-based bang-bang-control is able to achieve excellent results, taking the magnetic field energy into account. This demands for an amplifier with 'freerun-mode'. A current optimal control is able to run the punch machine with good results with minimal requirements of the current amplifier. The two methods show superior results compared to those using standard energy-based bang-bang or PID control.

The evaluation of the developed control methods on the test rig proposed in [15] and their performance during the punching process will be part of future work. Besides the test rig, which is able to store energies up to 50 J, the prototype of a resonance punch machine will be deployed.

6 REFERENCES

[1] Presz, W.; Andersen, B.; Wanheim, T.: Piezoelectric Driven Micro-press for Microforming, Institute of Materials Processing, Warsaw University of Technology, Journal of Achievements in Materials and Manufacturing Engineering, Vol. 18, Issue 1-2, 2006.

[2] Burt, W.C.: High Impact Electro Press, United States Patent US-5386205, 1995.

[3] Doherty, N. R.: Electrically Actuated Punch Press. United States Patent US3709083, US-4022090, 1973.

[4] Netronics Research and Developement, Ltd., New Milford, USA. etronicsresearch.com, 02.07.2015.

[5] Schulze Niehoff, H.; Vollertsen, F.: Versatile Microforming Press, Int. J. Materials and Product Technology, Vol. 32, No. 4, 2008.

[6] Schepp, F.: Linearmotorgetriebene Pressen für die Stanztechnik, Institut für Produktionstechnik und Umformmaschinen, Technische Universität Darmstadt, doctor thesis, 2001.

[7] Schneider, R.: Entwicklung einer Methode zur Optimierung von Fertigungsmaschinen für die Mikroumformtechnik am Beispiel von Linearmotorpressen, Institut für Produktionstechnik und Umformmaschinen, Technische Universität Darmstadt, doctor thesis, 2004.

[8] Dagen, M.; Riva, M. H.; Heimann, B.; Ortmaier, T.; Wager, C.; Krimm, R.; Behrens, B.-A.: A Multi-Axial Electromagnetically Actuated Punch for Cutting Micro-Components, Proceedings of the 2012 American Control Conference (ACC 2012), Montréal, Canada, 2012.

[9] Dagen, M.; Heimann, B.; Javadi, M.; Behrens, B.-A.: Design and Control of an Electromagnetically Actuated Punch, Proceedings of the 17th IFAC World Congress (IFAC 2008), Seoul, Korea, 2008.

[10] Dagen, M.; Abdellatif, H.; Heimann, B.: Applying Iterative Learning Control for Accuracy Improvement of an Electromagnetically Actuated Punch, Motion and Vibration Control (MOVIC 2008), 2008.

[11] Riva, M. H.; Dagen, M.; Ortmaier, T.: Adaptive High-Gain Observer for Joint State and Parameter Estimation: A Comparison to Extended and Unscented Kalman Filter, Proceedings of the 19th IFAC World Congress (IFAC 2014), Cape Town, South Africa, 2014.

[12] Bruderer AG, product bruchure BSTA 200,bruderer.com/uploads/tx_webruderer/BSTA-200_en_02.pdf, 02.07.2015.

[13] Yamada Dobby Europe Ltd., product brochure NXT-series, yamadadobby.com/downloads/nxt_spec_en.pdf, 02.07.2015.

[14] Banavar, R. N.; Mahindrakar, A. D.: Energy-based Swing-up of the Acrobot and Time-optimal Motion, Proceedings of IEEE Conference on Control Applications, vol. 1, pp. 706–711, 2003.

[15] Ahrens, M.; Hasselbusch, T.; Dagen, M.; Behrens, B.-A.; Ortmaier, T.: Development of a Miniaturized, Electromagnetically Actuated Punch, Proceedings of the ASME 2015 International Mechanical Engineering Congress & Exposition (IMECE2015), Houston (USA), November 2015.

Author: Ahrens, Markus

University: Leibniz Universität Hannover

Department: Institute for Mechatronic Systems

E-Mail: markus.ahrens@imes.uni-hannover.de